

*Pres. at 18th European Symp. on  
Semiconductor Detectors, New Development  
on Radiation Detectors, Schloss Elmau, Germany  
14-17 June 1998*

BNL - 65637

CONF-980676--

CHARGE COLLECTION AND CHARGE PULSE FORMATION  
IN HIGHLY IRRADIATED SILICON PLANAR DETECTORS\*

B. Dezillie and Z. Li

Brookhaven National Laboratory  
Upton, NY 11973

V. Eremin

A.F. Ioffe Physico-Technical Institute of Academy of Science of Russia  
194021 St. Petersburg, Russia

RECEIVED  
AUG 04 1998  
OSTI

June, 1998

DISTRIBUTION OF THIS DOCUMENT IS UNLIMITED

MASTER

\*This work was supported in part by the U.S. Department of Energy: Contract No. DE-AC02-98CH10886.

## **DISCLAIMER**

**Portions of this document may be illegible electronic image products. Images are produced from the best available original document.**

## **DISCLAIMER**

This report was prepared as an account of work sponsored by an agency of the United States Government. Neither the United States Government nor any agency thereof, nor any of their employees, makes any warranty, express or implied, or assumes any legal liability or responsibility for the accuracy, completeness, or usefulness of any information, apparatus, product, or process disclosed, or represents that its use would not infringe privately owned rights. Reference herein to any specific commercial product, process, or service by trade name, trademark, manufacturer, or otherwise does not necessarily constitute or imply its endorsement, recommendation, or favoring by the United States Government or any agency thereof. The views and opinions of authors expressed herein do not necessarily state or reflect those of the United States Government or any agency thereof.

# Charge Collection and Charge Pulse Formation in Highly Irradiated Silicon Planar Detectors\*

B. Dezillie and Z. Li  
Brookhaven National Laboratory, Upton, NY 11973, USA

V. Eremin  
A.F. Ioffe Physico-Technical Institute of Academy of Science of Russia, St. Petersburg, Russia

\*This investigation was done as a part of work established by the U.S. Department of Energy: Contract No: DE-AC02-98CH10886.

## Abstract

The interpretation of experimental data and predictions for future experiments for high-energy physics have been based on conventional methods like capacitance versus voltage (C-V) measurements. Experiments carried out on highly irradiated detectors show that the kinetics of the charge collection and the dependence of the charge pulse amplitude on the applied bias are deviated too far from those predicted by the conventional methods.

The described results show that in highly irradiated detectors, at a bias lower than the real full depletion voltage ( $V_{fd}$ ), the kinetics of the charge collection (Q) contains a fast and a slow component. At  $V = V_{fd}^*$ , which is the "full depletion voltage" traditionally determined by the extrapolation of the fast component amplitude of Q versus bias to the maximum value or from the standard C-V measurements, the pulse has a slow component with significant amplitude. This slow component can only be eliminated by applying additional bias that amounts to the real full depletion voltage ( $V_{fd}$ ) or more.

The above mentioned regularities are explained in this paper in terms of a model of an irradiated detector with multiple regions. This model allows one to use C-V, in a modified way, as well as TChT (transient charge technique) measurements to determine the  $V_{fd}$  for highly irradiated detectors.

## 1. Introduction

One of the main requirements for detectors used in high energy physics is their operation at full depletion mode that must attenuate the dependence of the signal amplitude on the properties of the Si detector sensitive volume. In this case, the signal must contain just one fast (or drift) component. It has been shown that the concentration of the deep acceptors, which acts as compensating centres, increases with the fluence. Consequently, the initial n-type Si with an initial resistivity of 1.5 k $\Omega$  cm becomes heavy compensated and the sign of the space charge in the active volume of the detector converses from positive to negative (space charge sign inversion, or SCSD). Additionally, the concentration of the space charge increases in time. In order to minimise the signal deficit of the detector after irradiation, the detector must operate at increased bias and stay fully depleted. In this case only the trapping effect will reduce the amplitude of the signal. In this report, the difficulties of the  $V_{fd}$  measurements using the two main methods (capacitance versus voltage and Transient Charge Technology (TChT)) will be discussed.

## 2. Samples and experimental conditions

For the experiments on the  $V_{fd}$  determination and the charge pulse formation, several planar detectors from the same silicon float-zone (FZ) wafer (# 595) with an initial resistivity of 1.5 k $\Omega$  have been used. The detector thickness (d) is 250  $\mu$ m and the initial  $V_{fd}$  is 120 V. An optic window of 2 mm diameter

in the Al metallization was made on both sides of the detector in order to allow easy laser injection. The detectors have been irradiated up to  $5 \times 10^{14}$  n/cm<sup>2</sup> by fast neutrons within 24 hours at the University of Massachusetts at Lowell (USA).

Full depletion voltage measurements were performed by the C-V and TChT methods. The C-V set-up contains a Keithley 487 High Voltage Source Measuring Unit and a Hewlett Packard 4263A Impedance Analyser operating at 10 kHz or 100 kHz.

TChT measurements were realised by laser injection, which generates non-equilibrium electron-hole pairs at a depth of about 10  $\mu$ m in the Si layer. The laser wavelength is 670 nm and the laser pulse duration is about 0.7 ns. A switch to a 50  $\Omega$  resistance allows one to measure the current pulse shape, or to the input capacitor of 2000 pF capacitance allows one to integrate the collected charge. The TChT set-up is illustrated Fig. 1. Details of the TChT set-up can be found in ref. [1].

### 3. Model

The model of Si detectors processed from n-type silicon and irradiated by fast neutrons up to fluences high enough ( $\Phi > 10^{13}$  n/cm<sup>2</sup>) for SCSI in the Space Charge Region (SCR) of the detector will be discussed. For simplicity, we will consider only three levels in the forbidden gap of the silicon detector: shallow donors ( $N_D$ ), shallow acceptors ( $N_A$ ) and deep acceptors ( $N_t$ ). These deep acceptors, introduced by radiation, compensate the initial n-type silicon.

The potential distribution in such a detector (after SCSI) under reverse applied voltage is shown in Fig. 2. Starting from the n<sup>+</sup>-“p” junction we can distinguish four layers in the structure:

- I) The Space Charge Region (SCR) with net effective concentration ( $N_{\text{eff}} \sim N_t$ ) of ionised donors and acceptors.
- II) The Quasi Neutral Region (QNR) for which the energy of the deep trap (acceptor) is higher than the Fermi level ( $E_F$ ) and therefore the filling of the deep level changes from the near filled condition in the space charge region to the steady-state level, which is specific for the neutral bulk [2-3]. Their conductivity will be significantly decreased compared to the neutral bulk as the gap between  $E_F$  and  $E_V$  (Energy of the Fermi level and the Valence band) is higher than in the bulk. Therefore, in a first approximation, the conductivity can be considered as zero. The thickness is estimated as the Debye length [2] in the bulk silicon with deep levels for the potential difference of  $E_F - E_t$ .
- III) The Electric Neutral Bulk (ENB) with the conductivity determined by the  $E_F$  position, which is nearly intrinsic. The applied bias to the ENB is a potential drop caused by the bulk leakage current.
- IV) The layer adjacent to the p<sup>+</sup> contact, which is originated by diffused holes from the heavy doped p<sup>+</sup> contact to the neutral base due to Fermi level difference between the p<sup>+</sup> contact and ENB ( $\sim 0.55$ eV) [4-5]. We denote this region as the enriched region (ENR). The depth of ENR is controlled by Debye length, which is reduced by the deep level trap concentration [6].

The characteristics of these four layers are summarised in Table 1.

This model of the heavy irradiated detector can be easily analysed by the equivalent circuit as illustrated in Fig. 3. In the figure,  $C_{\text{SCR}}$  is the capacitance of SCR;  $C_{\text{QNR}}$  is the capacitance of QNR, which is considered as an insulator;  $C_{\text{ENB}}$  in parallel with  $R_{\text{ENB}}$  gives the equivalent R-C circuit of ENB, which is equal to the Maxwell relaxation constant:

$$\tau_{\mu} = \frac{\varepsilon \varepsilon_0}{\mu e p} \quad (1)$$

where  $\varepsilon$  is the dielectric constant of Si,  $\varepsilon_0$  the permittivity of vacuum  $\mu$  the carrier mobility, and  $e$  the electronic charge.  $C_{ENR}$  in parallel with  $R_{ENR}$  gives the equivalent R-C circuit of ENR.

According to this equivalent circuit, the capacitance measured at the frequency  $\omega = 2\pi f$  can be approximated as the following:

$$\frac{1}{C} = \frac{1}{C_{SCR}} + \frac{1}{C_{ENB}} \sim W_{SCR} + W_{QNR} = W \quad (2)$$

assuming that  $\omega < \frac{1}{R_{ENB} C_{ENB}} \cong 10^7 \text{ s}^{-1}$ , which is the case for intrinsic ENB (200 k $\Omega$ -cm) observed in irradiated silicon [5]. Compared to the neutral bulk, the conductivity of the enriched region is increased by diffused holes and the contribution of ENR to capacitance can be neglected.

In this equation, only  $W_{SCR}$  is dependent on the reverse bias. The value  $W_{QNR}$  stays constant when the bulk current is stable or small enough not to change the steady-state potential distribution in the quasi-neutral region.

The simulated plot of  $W$  ( $W \sim 1/C$ ) as a function of square root of bias (see Fig. 4, it is equivalent to  $1/C$  vs.  $\sqrt{V}$ ) illustrates that one can separate  $W_{SCR}$  from  $W_{QNR}$  using Eq. 2. In the figure,  $W_{QNR}$  (or  $1/C_{QNR}$ ) is determined by the Y-axis intersection of the curve  $W(V)$ . It is clear that a mistake occurs when one determines the  $V_{fd}$  by the traditional method of extrapolating the C-V curve to the point of the capacitance saturation value, which gives a false value of full depletion voltage,  $V_{fd}^*$ . The correct result of  $V_{fd}$  can be obtained by 1) determining  $1/C_{QNR}$  from the plot  $\frac{1}{C} = f(\sqrt{V})$ , 2) subtracting  $1/C_{QNR}$  from  $1/C$ , and 3) re-plot  $1/C' = 1/C - 1/C_{QNR}$  vs.  $\sqrt{V}$  and of extrapolating curve to the point of the capacitance saturation value to get  $V_{fd}$ , as shown in Fig. 4.

This model allows us to describe the main peculiarities of the charge pulse response  $Q(t)$  for two cases: non-equilibrium pairs generation near the  $p^+$  and  $n^+$  contacts.

a) Generation near the  $n^+$  contact (at the high field side):

In this case, the carriers are promptly generated in the high electric field and they start drifting immediately. Holes, drifting first through the SCR and then into the quasi-neutral region, will cause induced charge with a value according to the Ramos theorem:

$$Q_{fast} = Q_0 \frac{W_{SCR}}{d} \quad (3)$$

Where  $Q_0$  is generated charge.  $d$  the detector thickness. The rising time can be estimated as a time constant of charge collection for the SCR ( $\tau_{SCR}$ ):

$$\tau_{SCR} = \frac{1}{\mu_p e N_{eff}} \quad (4)$$

The time spent by holes passing the QNR can be estimated in the first approximation:

$$\tau_{QNR} = \frac{W_{QNR}^2}{\mu_p V_{QNR}} \quad (5)$$

In general,  $\tau_{QNR}$  is much larger than  $\tau_{SCR}$  due to very small potential drop in QNR ( $V_{QNR}$ ).

The holes coming into the neutral bulk will be injected to the  $p^+$  contact by the flow of the ohmic current in the ENB [1], which leads to the slow component in  $Q^n(t)$ . The time constant of this process is larger than drift times in SCR and QNR and can be estimated from the Maxwell time ( $\tau^M = \epsilon\epsilon_0\rho$ ) for the ENB as the following:

$$\tau_{ENB} = \tau_{ENB}^M \frac{d}{W_{SCR} + W_{QNR}} = \epsilon\epsilon_0\rho_{ENB} \frac{d}{W_{SCR} + W_{QNR}} \quad (6)$$

Consequently, the amplitude of this slow component is:

$$Q^{n,sl} = Q_0 \frac{W_{ENB}}{d} \quad (7)$$

The region adjacent to the  $p^+$  contact enriched by holes (ENR) will not effect the charge pulse formation as their effective resistivity (the average value over this region) and  $\tau_{ENR}^M$  is significant lower than the one in the ENB.

b) Generation at the  $p^+$  contact (at the low electric field side) as shown in Fig. 5:

The movement of the generated carriers (electrons) in the built-in field of the free carrier enriched region near the  $p^+$  contact forms a fast component at the charge pulse. Consequently, the charge collected during this process will be proportional to the width of  $W_{ENR}$  as:

$$Q_{fast}^p = Q_0 \frac{W_{ENR}}{d} \quad (8)$$

Since  $W_{ENR}$  does not depend on the  $V_B$ , this fast signal must stay stable in the whole range of the  $V_B$ . The specific time of this process estimated from  $\tau_{ENR}^M$  is in the ns range.

In the large time scale, there will be two processes complementary to the fast component:

- 1) The discharge of  $p-p^+$  layer so that the collected electrons in the  $p$ -bulk and holes in the  $p^+$  contact will recombine. It will lead to the decay of the charge pulse, just after it's rising.
- 2) The relaxation of electrons which come to the neutral bulk by the current flow through the QNR and the SCR. This process is equivalent to the charge collection process as described previously for the slow component (Eq. 7) and will lead to a slow rising of the charge pulse (see Fig. 6).

The time constant of the slow component can be estimated from Eq. 6 (in the order of a few  $\mu s$ ).

## 4. Experimental data

### 4.1 C-V technique

The C-V data re-plotted as  $W$  versus  $V^{1/2}$  is shown in Fig. 7. The value  $W$  is calculated as the following:

$$W = \frac{\varepsilon \varepsilon_0 A}{C} \quad (9)$$

Where  $A$  is the area of the  $n^+/p$  junctions. The curve from Fig. 6 correlates well to the model (see Fig. 4) and is approximated by a linear fit in the full range of the bias. The intersection of the fitted line with the Y-axis gives the thickness of the quasi-neutral region  $W_{QNR} = 21 \mu\text{m}$ . Extrapolation of the fit to the detector thickness gives a false full depletion voltage ( $V_{fd}^* = 462 \text{ V}$ ) as it was determined before. Note that it is exactly the same approach for full depletion voltage measurement used in most works by extrapolation of  $\log(C)$  versus  $\log(V)$  plot (Fig. 8) to the geometrical capacitance  $C_{fd}$  [7].

The value of  $V_{fd}^*$  is a voltage when the quasi-neutral region just touches the  $p^+$  contact of the detector. Hence, it can not be considered as the real  $V_{fd}$  as it is not enough for the collection of the whole charge. The real value of  $V_{fd}$  is higher, and according to Eq. (2), can be determined by shifting the fit line parallel to the right, passing the origin. The value of the corrected  $V_{fd}$  is 529 V. This value is 14.5% higher than  $V_{fd}^*$ . The other examples see in ref. [8].

#### 4.2 The Transient Charge Technique (TChT)

In the case that the light coming on the  $n^+$  contact as shown in Fig. 9 (the high field side), the charge pulses have two components; a fast one and a slow one. The amplitude of the fast component increases with the bias according to Eq. 3. The slow component decreases in rise time and in amplitude with bias according to Eq. 6 and 7.

In the case of non-equilibrium carrier excitation at the  $p^+$  side (the low electric field), the experimental charge pulses (see Fig. 10 and 11) at the low biases are very similar to the shapes predicted by our model (see Fig. 5). The plot of the fast component amplitude vs. bias (see Fig. 12) shows a slow rising part at biases below the  $V = 300 \text{ V}$ . The value of  $W_{ENR}$  can be estimated from the ratio of the amplitude of this slow rising part and the overall amplitude, which gives  $W_{ENR} \sim (50/2400) \cdot d \cong 5 \mu\text{m}$ .

The fast increasing part of  $Q_{fast}^p(V)$  at biases larger than 300 V is more complicate compared to the model. It contains two parts with significantly different slopes (see detail of Fig. 12). The linear extrapolation of the fast growing part of this curve to the maximum of  $Q_{fast}^p$  gives a value of  $V_1 \sim 445 \text{ V}$ . The slow part that follows reaches the maximum of  $Q_{fast}^p$  at  $V_2 = 533 \text{ V}$ . The plot of the linear fits of this two parts of  $Q_{fast}^p(V)$  together with the extracted values are shown in the detail of Fig. 10.

The values of  $V_1$  and  $V_2$  are very close to those of  $V_{fd}^*$  and  $V_{fd}$ , measured by the C-V method, respectively. This good correlation allows us to consider the process of the charge pulse formation for highly irradiated Si detectors in two parts. The first part occurs during the reduction of the ENB thickness under increased bias (the fast rising part in the  $Q_{fast}^p(V)$  curve) and stops at  $V_1$  when the QNR starts touching the back contact. According to the model the second part of  $Q_{fast}^p(V)$  corresponds to the shift of the SCR border to the  $p^+$  contact by the reduction of the  $W_{QNR}$ . The charge collection deficit of about  $(100/2400) \cdot 100 \cong 4\%$  is diminished by increasing of the bias up to 533 V during this second part.

#### 5. Conclusions

1. The proposed model for heavy irradiated Si detectors allows one to explain the main regularities observed in the C-V and TChT experiments.
2. The approach of the C-V data treatment in this work provides a modified way to determine the real full depletion voltage  $V_{fd}$  for highly irradiated detectors. In addition, it allows one to estimate the influence of a deep level on the electric field distribution on the SCR border.
3. The results of the C-V measurements are well verified by the TChT experiment. The slow rising component of  $Q_{fast}^p(V)$  is explained quantitatively by the proposed model.

4. The experiments carried out show that the slow component of  $Q(V)$  could have two origins: The existing of the QNR and the trapping/de-trapping originated by deep traps. The comparison of C-V and TChT experiments allows us to separate these two effects.

## References

- [1] V. Eremin et al., "Development of transient current and charge techniques for the measurement of effective net concentration of ionised charges ( $N_{\text{eff}}$ ) in the space charge region of p-n junction detectors", Nucl. Instr. and Meth. A 372 (1996) 388-398.
- [2] V. Eremin et al., "Capacitance peculiarity of p-i-n structures with deep levels", Sov. Phys. and Techn. of Semiconductors, Vol. 9, No. 1, p. 95, 1975.
- [3] Z. Li and H. W. Kraner, "Fast Neutron Radiation Effects on High Resistivity Silicon Junction Detectors", Journal of Electr. Materials, Vol. 21, No. 7, 1992.
- [4] V. Eremin and Z. Li, " Determination of the Fermi Level Position for Neutron Irradiated High Resistivity Detectors and Materials Using the Transient Charge Technique (TChT)", IEEE Trans. on Nucl. Science, Vol . 41 No. 6, Dec 1994.
- [5] Z. Li, "Elevated Temperature Annealing of Bulk Resistivity of Neutron Irradiated Detector Grade Silicon Planar Detectors". NIM Phys. Res. A 368, p.353-363, 1996.
- [6] N. Derhacopian and N.M. Haegel, "Experimental study of transport in a trap-dominated relaxation semiconductor", Phys. Rev. B, Vol. 44, No. 23, p. 44, 1991.
- [7] A. Chilingarov, "Systematic Effects in Measurements of the Depletion Voltage", DESY-PROCEEDINGS-1999-02, Presented at the 3<sup>rd</sup> ROSE Workshop on Radiation Hardening of Silicon Detectors, DESY Hamburg, 12-14 February 1998.
- [8] B. Dezillie, V. Eremin and Z. Li, "Defect analysis of silicon detectors made of different materials for radiation hardness:, BNL-65394 and to be published in NIM Phys. Res. A, (Proceedings of the 2<sup>nd</sup> International Conference on Radiation Effects on Semiconductor Materials, Detectors and Devices, Florence, Italy, March 4-6, 1998).

**Table caption**

Table 1      The characteristics of the four layers in a silicon structure.

Layer	Free carrier concentration	Net effective Concentration	Potential drop	Layer thickness
SCR	$\sim 0$	$N_D^+ - N_A^- - N_t^-$	$V_B + \Phi_c -  E_F - E_t $	$W^{SCR} = \sqrt{\frac{2 \epsilon \epsilon_0 (V + V_{bi})}{e N_{eff}}}$
QNR	$\sim 0$	$p \sim n_I$	$E_F - E_t$	$W^{QNR} = \sqrt{\frac{2 \epsilon \epsilon_0 (E_p - E_t)}{e p}}$
ENB	$p \sim n_i$	0	$j_r \rho (d - W_{SCR} - W_{QNR} - W_{ENB})$	$d - W_{SCR} - W_{QNR} - W_{ENB}$
ENR	$\gg n_i$	$\gg n_i$	$E_p^+ - E_F$	$W = \frac{L_D}{\sqrt{1 + \frac{N_t}{p}}}$

## Figure caption

Fig.1 Schematic of the TChT set-up.

Fig. 2 The potential distribution in a highly irradiated detector under reverse voltage (+V) to the n<sup>+</sup> contact.

Fig. 3 Equivalent schematic of the model. The sequence of the elements corresponds to the sequence of the regions in Fig. 2.

Fig. 4 The drawing of the thickness versus  $V^{1/2}$  shows the standard data treatment approach gives  $V_{fd}^*$ , which is less than the real  $V_{fd}$  determined from the replotted line.

Fig. 5 Electric field distribution in highly irradiated detectors at  $V < V_{fd}$ .

Fig. 6 The drawing of the charge pulse for the of electron-hole pair generation at the low field contact (p<sup>+</sup> contact in the model).

Fig. 7 The thickness measured as a capacitance of the detector and the replotted data versus  $V^{1/2}$ .

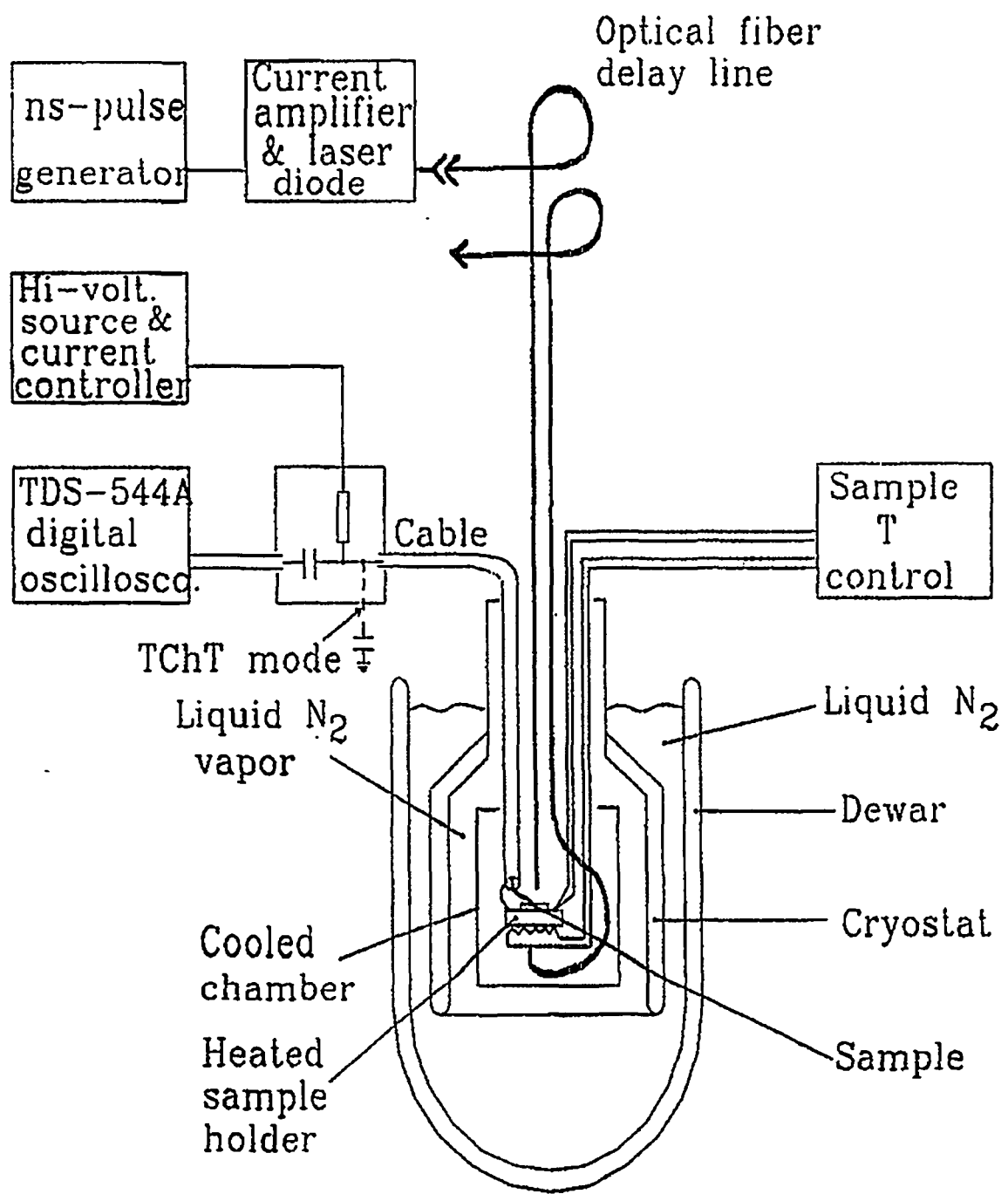
Fig. 8 Traditional treatment of C-V data.

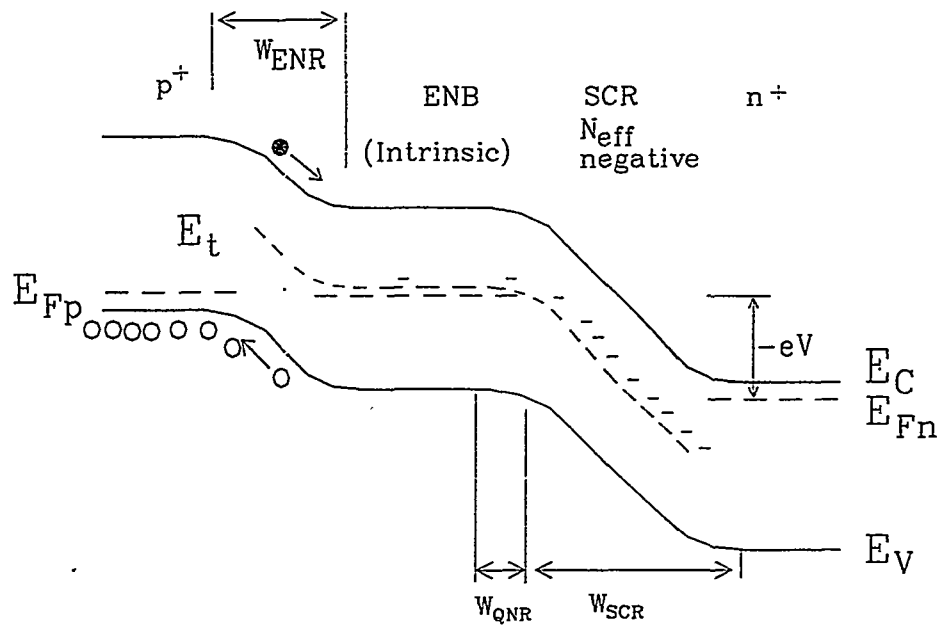
Fig. 9 The charge pulses for electron collection at different biases.

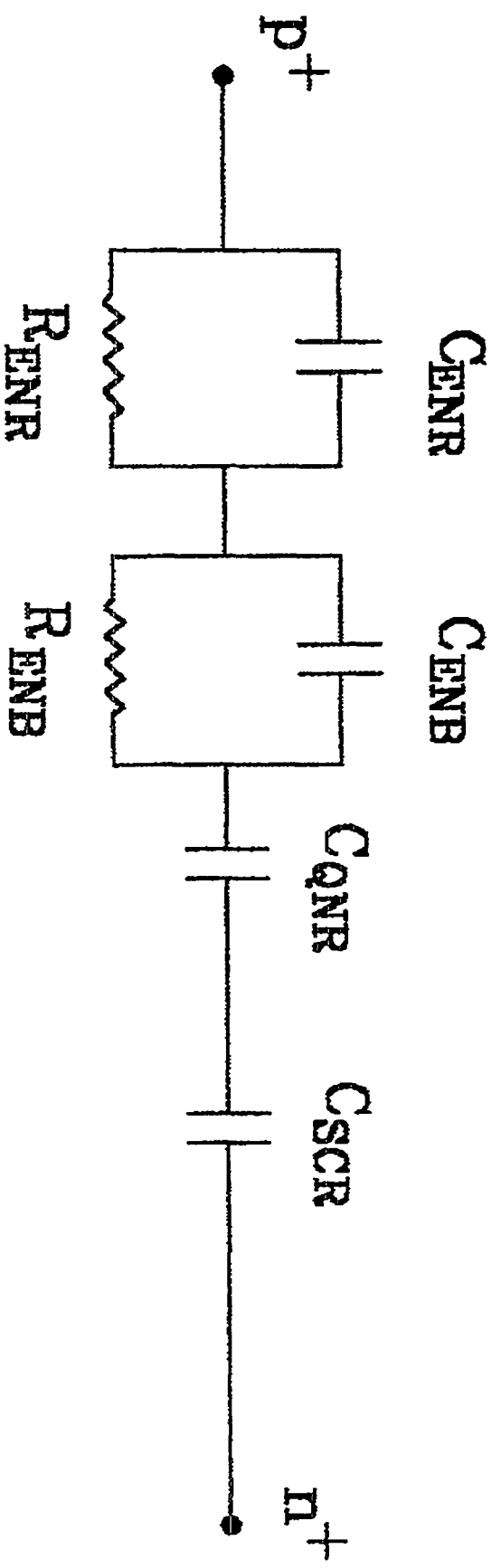
Fig. 10 The charge pulse for hole collection at different biases in the full range of bias.

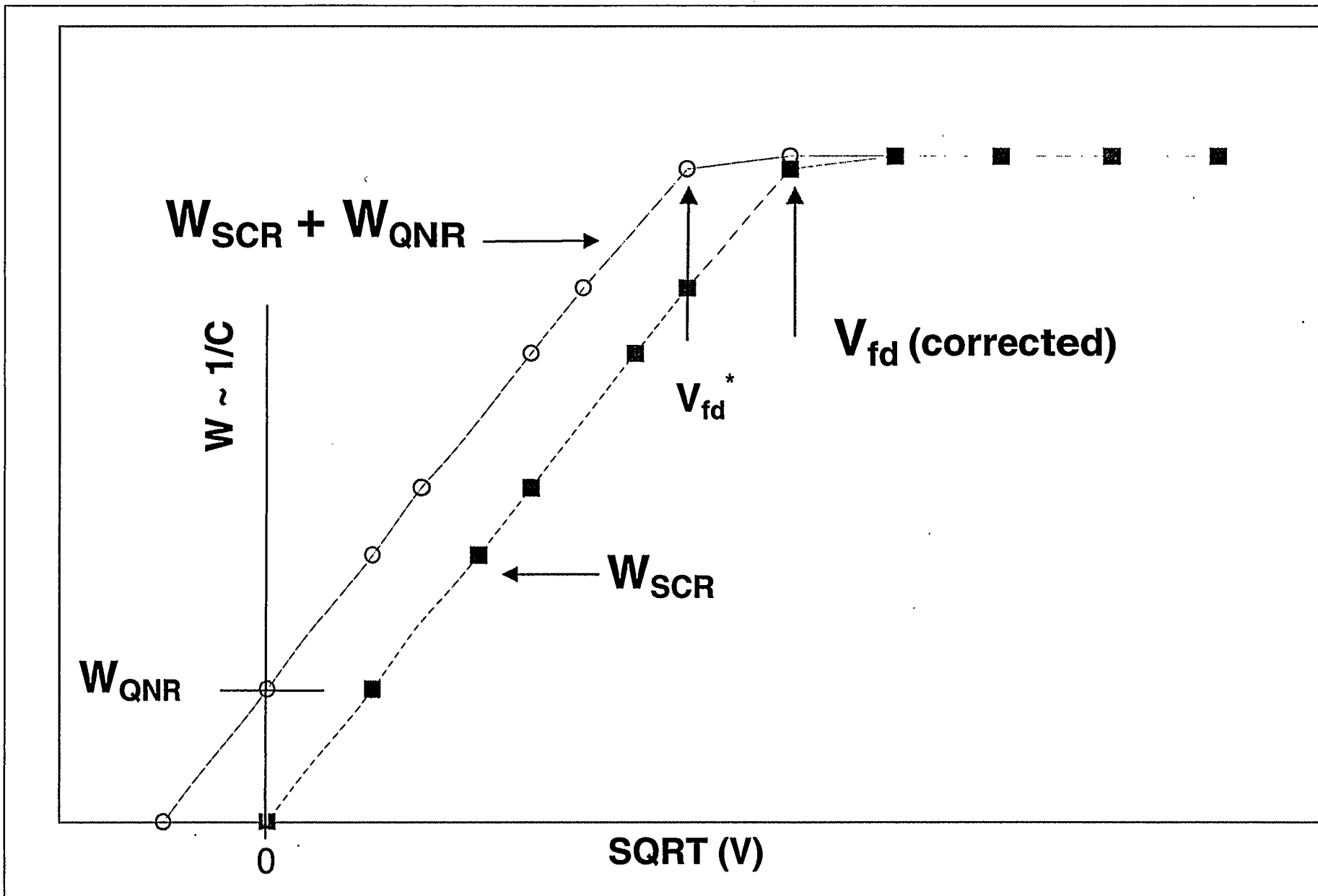
Fig. 11 The charge pulse for hole collection at different biases at low biases.

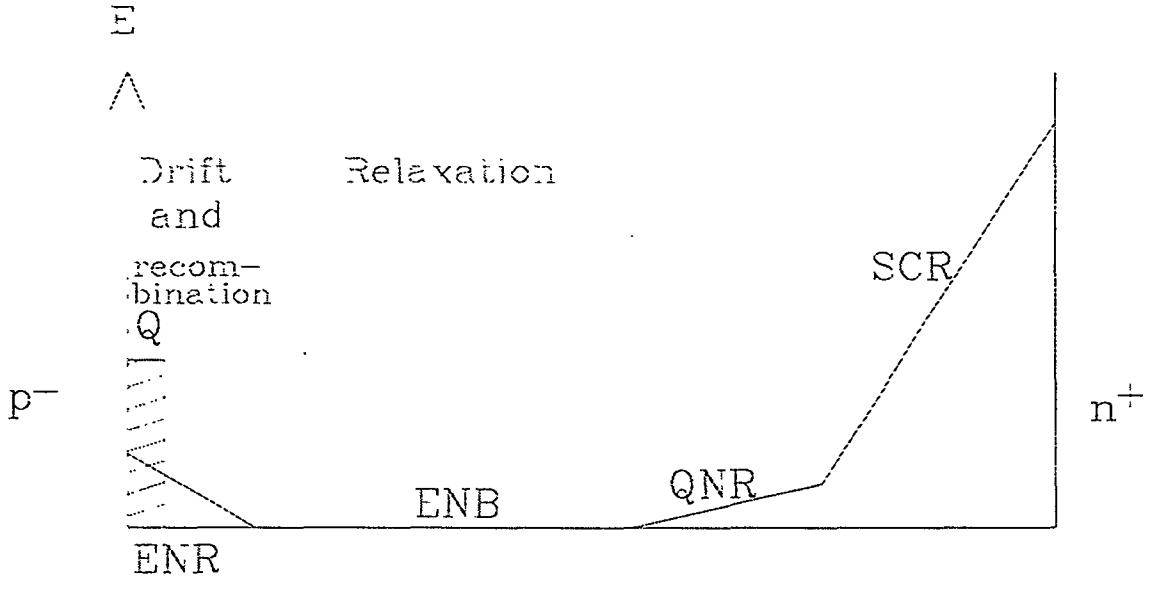
Fig.12 The fast component versus bias. The fragment shows the detail of the amplitude saturation and their fit lines.

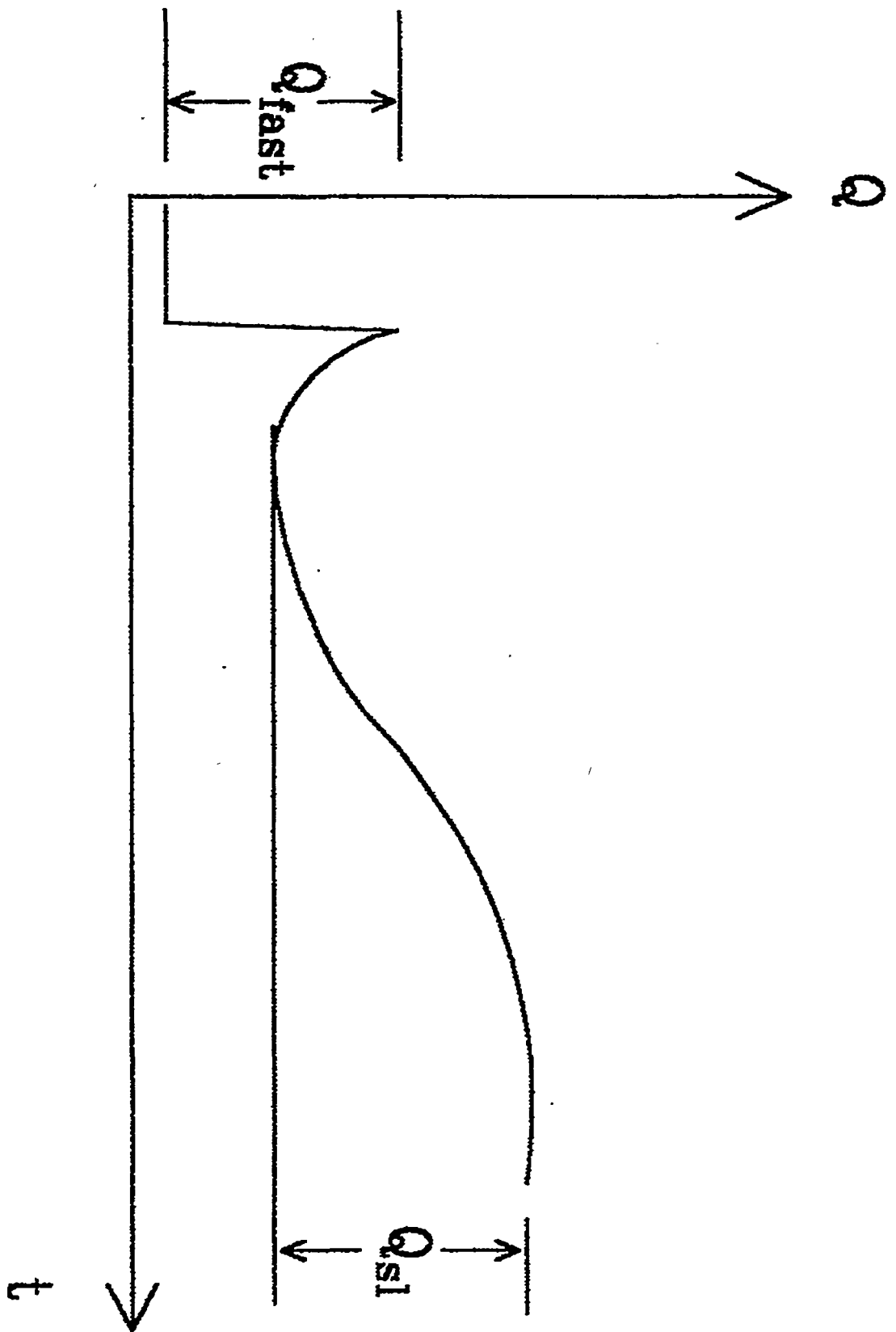












Thickness versus bias calculated from C-V measurement on a FZ silicon detector after 3500 days equiv. RT annealing

